

# The next generation humidity chamber for biological samples

## Biological measurements with neutron scattering: in warm and humid environments

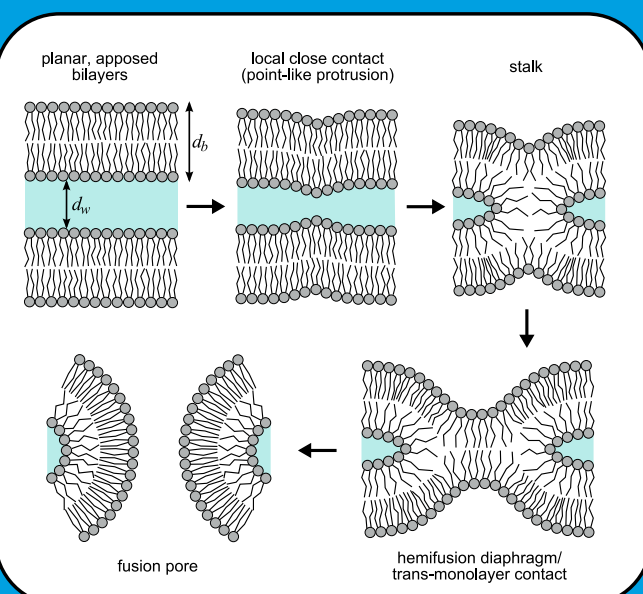


Figure 1. Pathway of lipid bilayer fusion.\*

Lipid bilayers form complex structures which vary dramatically with the temperature and relative humidity (r.h.) of their environment.

Stalk and fusion pore formation (normally protein mediated) is observed in bilayers by decreasing sample humidity (see Figure 1).

Phase diagrams show that certain lipid/sterol systems go through structural changes when humidity is varied (see Figure 2).

To determine phase diagrams of these systems, it is necessary to have an environment with a wide range of accessible humidities.

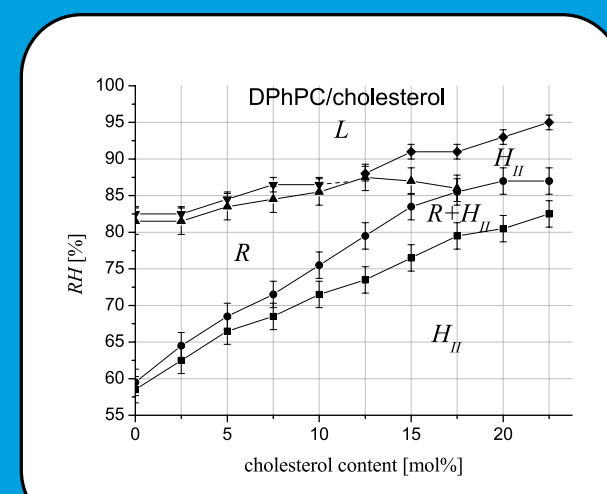


Figure 2. Phase diagram of DPhPC and Cholesterol mixture as a function of relative humidity and cholesterol content.\*

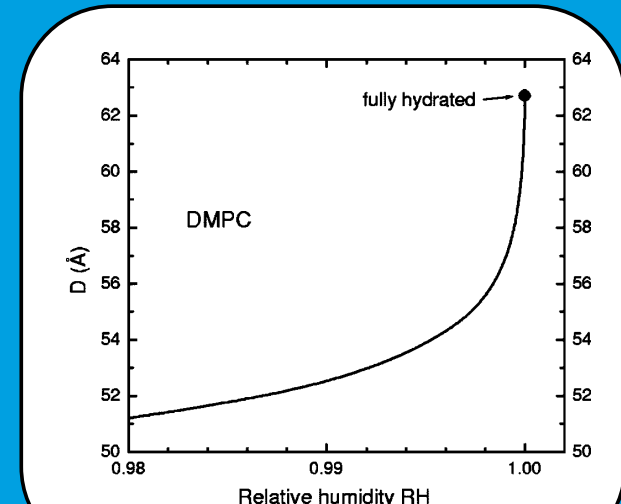


Figure 3. d-spacing of DMPC lipid bilayer for humidity values close to saturation.\*

Experiments at high humidities will provide a more realistic picture of the lipid bilayer behaviour in nature.

The dramatic dependence of d-spacing on humidity above 98% r.h. (see Figure 3) makes high r.h. region extremely interesting, but with today's humidity control techniques this region has been largely inaccessible.

## Today's generation of humidity controlled sample environments

### Saturated salt solution

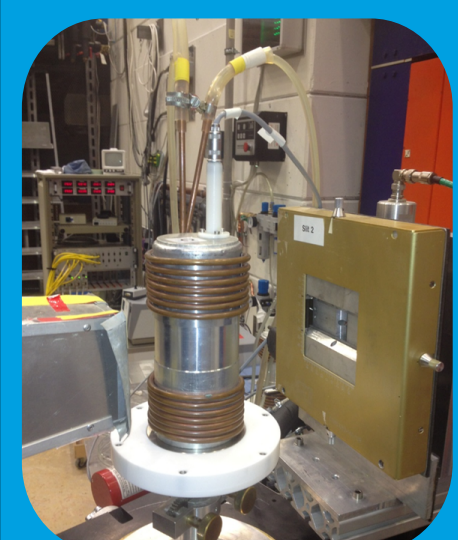


Figure 4. Saturated salt humidity chamber. Hauß, V1, HZB.

- ✓ precise and reliable (tables available)
- ✓ no calibration necessary
- ✗ discrete humidity steps
- ✗ slow equilibration times

### Gas vapour flow

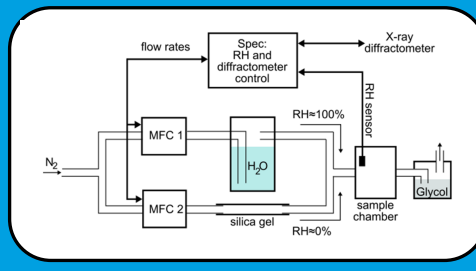


Figure 5. Humidity control setup Salditt, IRP.\*

- ✓ continuous humidity range possible
- ✓ automated humidity change (with mass flow controllers)
- ✓ fast equilibration time
- ✗ upper limit of humidity ~95%
- ✗ temperature gradients in cell or tubing could cause condensation

### Bulk water

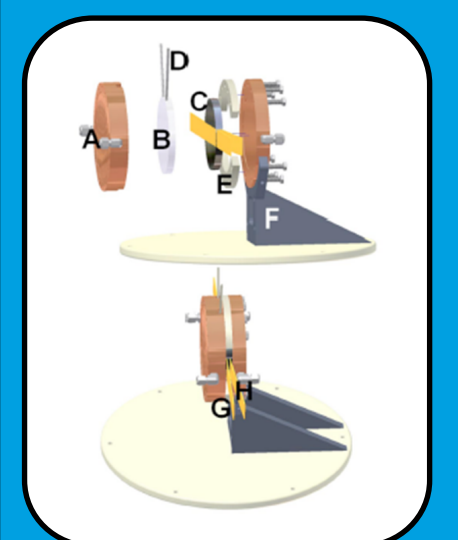


Figure 6. Reflectometry bulk water cell. Harroun, CINS.\*

- ✓ 100% relative humidity achievable
- ✓ quick deuterium contrast change in-situ
- ✗ sample loss to bulk solution (charged lipids)
- ✗ limited to reflectometry

### Temperature controlled

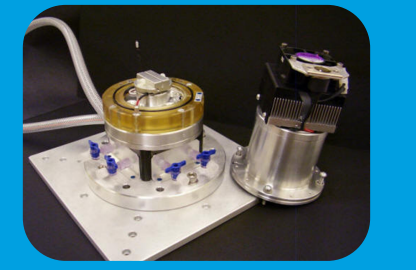


Figure 7. Temp. controlled cell Rheinstädter, McMaster.\*

- ✓ high (>95% r.h.) possible
- ✓ quick deuterium contrast in-situ
- ✗ temperature gradients (from Peltier or external) lead to condensation
- ✗ difficult to calibrate heaters for desired r.h.

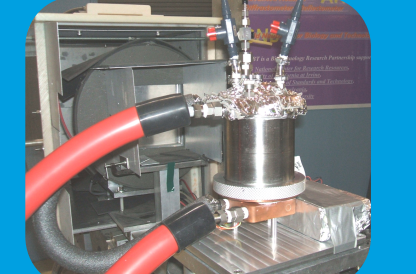


Figure 8. Temp. controlled cell. Heinrich, NIST.\*

## Finite element simulations

### Why use simulations?

- to check for problems with current design
- to test the working principle, observe what can be expected in the physical version
- to determine some calibration parameters (temperature targets for chillers) for faster progress later

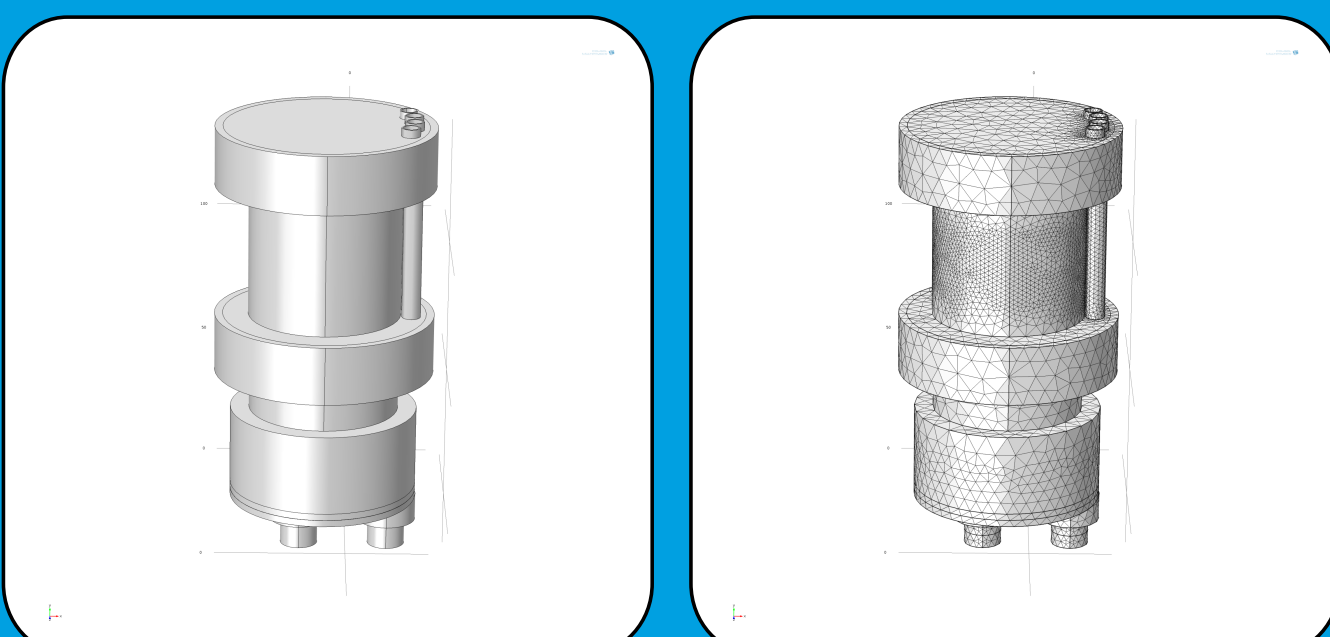


Figure 10. Steps in COMSOL Finite Elements simulation\*. Left: Inner cell of current CAD drawing imported, surfaces simplified, and materials assigned. Right: All surfaces divided into mesh of finite elements, elements make up entries in matrix. Initial and thermodynamic parameters defined and partial differential equations performed.

Upper and lower wire access ports for sensors (T or r.h.), Peltier heater

Wide angular scanning range (~300°)

Three water channels connect to three independent chillers - extreme temperature control

Simple sample change - remove entire upper cell

Further design steps to test: fan in inner cell, inverted sample holder, additional chiller, baffles between water bath and sample, solution change

Total size 240mm x Ø110mm compatible with common diffraction instruments

Double walled evacuated aluminum construction

Inner cell size 122mm x Ø50mm big enough for common samples, small enough for fast equilibration

Thermal decoupling of  
 - sample from lower cell  
 - inner cell from outer cell  
 - outer cell from instrument

Simple modifications would allow a variety of scattering geometries - sapphire windows for SANS, horizontal sample for reflectometry

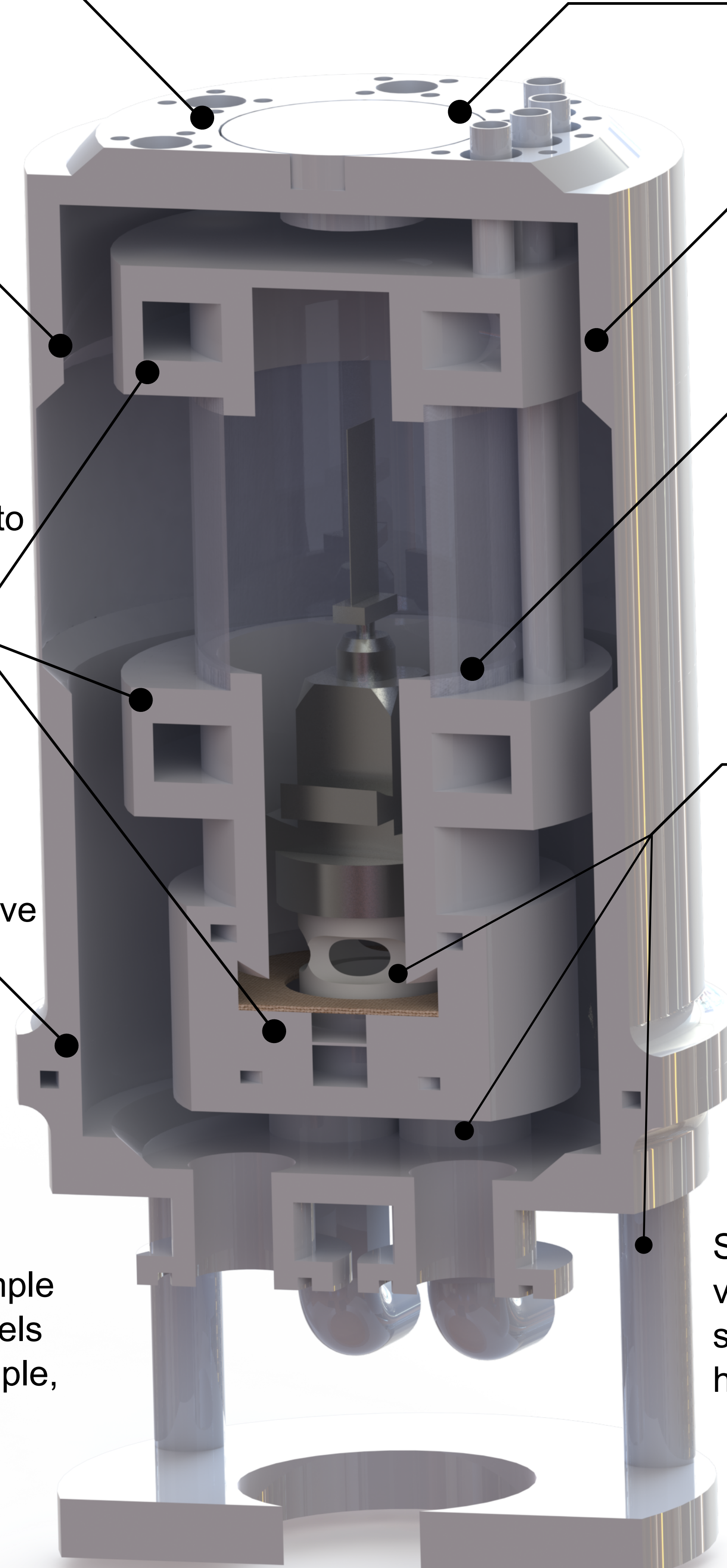


Figure 9. Three dimensional render of new humidity cell drawing. A. Perkins, ILL

## Humidity through temperature

- Relative humidity is calculated from partial vapour pressure and saturation vapour pressure (Eq. 1)

- Vapour pressure can be fully defined by the Antoine equation - depends only on temperature (Eq. 2)

- Through precise tempering of our humidity chamber (flowing water cooled in an isothermal bath through chiller channels) accurate humidity at the sample surface is achieved

$$r.h. = \frac{\text{partial vapour pressure}}{\text{saturation vapour pressure}}$$

Equation 1. Relative humidity calculated from vapour pressure.\*

$$\log_{10} \frac{P}{\text{bar}} = 5.402 - \frac{1838.7 \text{ K}}{T(K) - 31.7 \text{ K}}$$

Equation 2. Antoine equation with constants from Bridgeman.\*

### Simulation parameters

Sample target temperature = 298 K

Bottom chiller temperature is defined by relative humidity goal (through partial pressure and Antoine equation - Eq. 1&2).

Sample temperature target is achieved with two chiller loops above and below the sample.

Chiller temperatures selected to suppress cold temperature from water bath at the bottom of the cell and create uniform temperature (humidity) across sample surface.

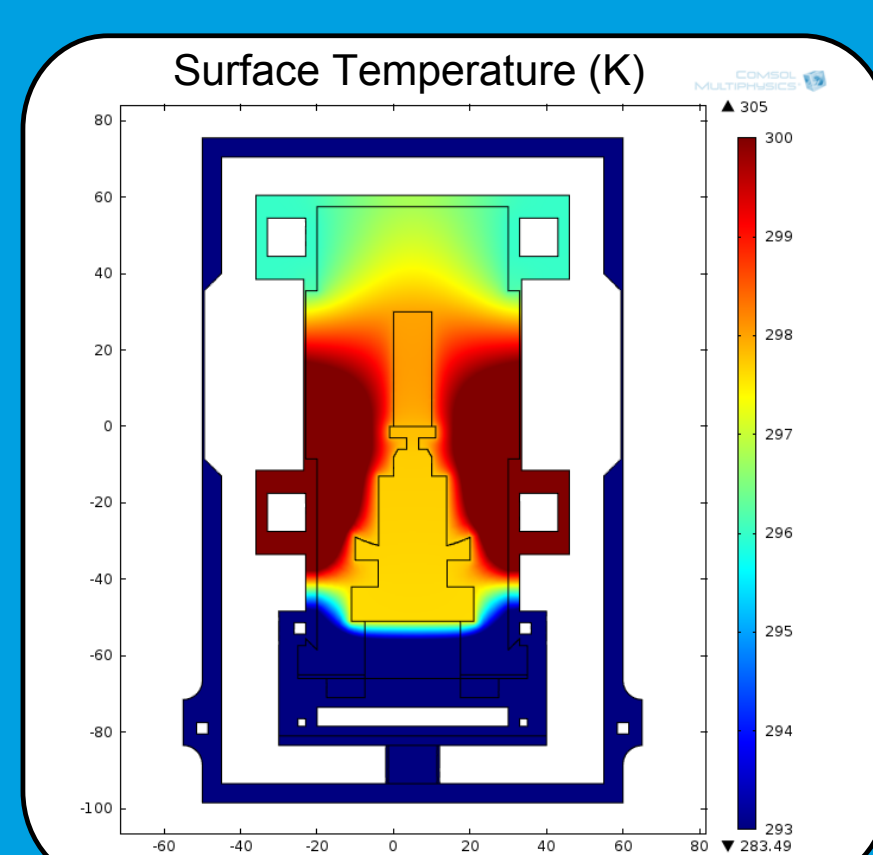


Figure 11. Equilibrium heat distribution across surfaces in COMSOL thermal simulation. Drastically low humidity situation shown for clarity with 40% relative humidity on sample, with water bath temperature 283.49 K and sample target 298 K.

### Performance of two independent chillers

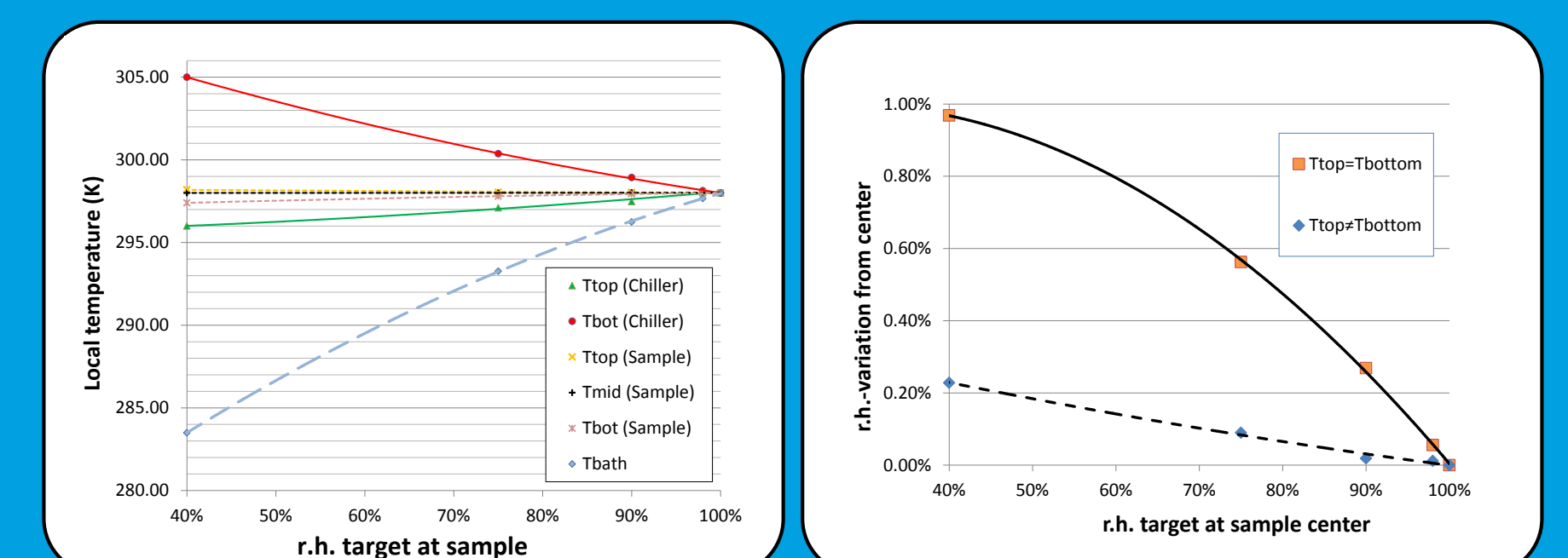


Figure 12. Results of COMSOL simulations. Left: Equilibrium temperature of three temperature independent chillers and at points along the sample surface for a range of humidity targets. Right: Calculated relative humidity difference from target humidity on sample surface with chillers above and below sample at the same temperature (orange) and at different temperatures (blue) to counter the effect of the cold bath below.

Relative humidity variation across the sample is reduced to 1/4 of the value when the temperature gradient is suppressed by two different chiller temperatures, compared to two chillers at the same temperature.

\*Aeffner et al., Membrane fusion intermediates and the effect of cholesterol: An in-house X-ray scattering study. Eur. Phys. J. E 30, 205-214 (2009)  
 \*Chu et al., Anomalous swelling of lipid bilayer stacks is caused by softening of the bending modulus. Phys. Rev. E 71, 041904 (2005)  
 \*Harroun et al., Variable temperature, relative humidity 0%–100%, and liquid neutron reflectometry... Rev. Sci. Instr. 76, 065101 (2005)  
 \*Perry, R.H. and Green, D.W., Perry's Chemical Engineers' Handbook (7th Edition), McGraw-Hill, ISBN 0-07-049841-5  
 \*Bridgeman, O.C.; Aldrich, E.W., Vapor Pressure Tables for Water, J. Heat Transfer 86, 279-286 (1964).  
 \*COMSOL Multiphysics 4.2a. COMSOL Inc., Palo Alto, CA.

